BRAIN
ORIGINAL ARTICLE

Sleep, pericyte subtypes and cognitive decline in adults with and without Alzheimer's disease

Mahnoor Hamid,[1,2] Trishna Saha Detroja,[1,2] Shreejoy J. Tripathy,[2,3,4,5] Vilas Menon,[6] Jishu Xu,[6,7] Lei Yu,[6,7] Yanling Wang,[6,7] Aron S. Buchman,[6,7] David A. Bennett,[6,7] Philip L. De Jager[8,9,10] and Andrew S. P. Lim[1,2]

Sleep fragmentation is common in older adults and is associated with cognitive impairment and dementia, as well as key histopathological correlates of dementia, including small vessel disease and cerebral infarcts. Vascular and blood–brain barrier dysfunction are thought to contribute to cognitive decline and dementia. Pericytes, a key vascular cell type, may play a key role.

In model organisms, sleep disruption is associated with pericyte dysfunction and blood–brain barrier breakdown. Recent advances in single-nucleus RNA sequencing (snRNAseq) technology have identified two transcriptionally distinct subtypes of pericytes: extracellular matrix protein-expressing M-pericytes and solute carrier-expressing T-pericytes. However, the relationship between sleep, pericyte biology and cognition in humans remains unclear.

We tested the hypothesis that differences in the composition of brain pericyte subpopulations, as inferred from marker gene expression, may link sleep fragmentation and cognitive decline. We leveraged two published human brain snRNAseq datasets to identify specific marker genes for M- and T-type pericytes. We then used post-mortem bulk RNAseq data from the dorsolateral prefrontal cortex ($n = 1092$) and lateral orbitofrontal cortex ($n = 495$) to quantify expression of these marker genes in older adults in two longitudinal cohort studies: the Religious Orders Study and Rush Memory and Aging Project. We derived trajectories of global cognitive function from participants' ante-mortem annual cognitive assessments, while sleep fragmentation was derived from ante-mortem wrist-actigraphy recordings from a subset of 572 participants. We used multivariate linear regression to relate pericyte marker gene expression to sleep fragmentation and cognitive decline in the decade preceding death.

In the dorsolateral prefrontal cortex, greater average sleep fragmentation was associated with greater expression of M-pericyte marker genes [estimate $= +3.65 \times 10^{-1}$, standard error (SE) $= 1.61 \times 10^{-1}$, $P = 0.024$] but not T-pericyte marker genes. Dorsolateral prefrontal cortex expression of M-pericyte (estimate $= -8.30 \times 10^{-3}$, SE $= 3.37 \times 10^{-3}$, $P = 0.014$) but not T-pericyte marker genes was associated with more rapid cognitive decline in the 10 years prior to death. In the lateral orbitofrontal cortex, greater sleep fragmentation was also associated with greater composite M-pericyte gene expression (estimate $= +4.48 \times 10^{-1}$, SE $= 1.92 \times 10^{-1}$, $P = 0.02$), which in turn was associated with faster cognitive decline in the decade preceding death (estimate $= -1.30 \times 10^{-2}$, SE $= 4.55 \times 10^{-3}$, $P = 0.0044$).

These findings identify a potential role of M-pericytes in linking sleep fragmentation and cognitive trajectories in older adults. Additionally, our findings highlight the importance of vascular mechanisms in linking disrupted sleep to dementia.

Received August 13, 2024. Revised February 10, 2025. Accepted March 29, 2025. Advance access publication July 14, 2025

1 Division of Neurology, Department of Medicine, Hurvitz Brain Sciences Program, Sunnybrook Health Sciences Centre, University of Toronto, Toronto, ON, Canada M4N 3M5
2 Institute of Medical Sciences, University of Toronto, Toronto, ON, Canada M5S 3K3
3 Krembil Centre for Neuroinformatics, Centre for Addiction and Mental Health, Toronto, ON, Canada M5T 2S8
4 Department of Psychiatry, University of Toronto, Toronto, ON, Canada M5T 1R8
5 Department of Physiology, University of Toronto, Toronto, ON, Canada M5S 1A8
6 Rush Alzheimer Disease Center, Rush University Medical Center, Chicago, IL 60612, USA
7 Department of Neurological Sciences, Rush University, Chicago, IL 60612, USA
8 Center for Translational & Computational Neuroimmunology, Columbia University Irving Medical Center, New York, NY 10032, USA
9 Department of Neurology, Columbia University Irving Medical Center, New York, NY 10032, USA
10 Department of Neurology, Taub Institute for Research on Alzheimer's Disease and the Aging Brain, NewYork, NY 10032, USA

Correspondence to: Andrew S. P. Lim
Division of Neurology, Department of Medicine, Hurvitz Brain Sciences Program
Sunnybrook Health Sciences Centre, 2075 Bayview Ave.
Room A4, Toronto, ON, Canada M4N 3M5
E-mail: Andrew.lim@utoronto.ca

Keywords: sleep fragmentation; cognitive decline; actigraphy; aging; cerebral small vessel disease

Introduction

Alzheimer's disease and related dementias (ADRD) are a leading cause of death among older adults, as well as a major contributor to disability and dependency.[1] Interventions to prevent cognitive impairment and ADRD are urgently needed. In older adults, sleep disruption and ADRD can coexist.[2,3] In some individuals, sleep disruption can precede the onset of cognitive impairment by years, with emerging evidence suggesting a bidirectional link between sleep disruption and ADRD.[4,5] However, the mechanisms underlying these links remain incompletely described.

Cerebral small vessel disease (CSVD), a term encompassing pathology of the small vessels of the brain, is an important pathological correlate of cognitive impairment in older adults.[6,7] Key elements of cerebral small vessels are pericytes—a type of mural cell embedded in the vessel basement membrane.[8,9] Pericytes are involved in regulating cerebral blood flow and maintaining the blood–brain barrier (BBB).[8,9] Pericyte dysfunction, indicated by increased shedding of soluble PDGFRβ from pericytes to the CSF, has been identified as an early feature of Alzheimer's disease pathogenesis.[10,11] A recent single nucleus RNA sequencing (snRNAseq) study of human brain vascular cells identified two transcriptionally defined subtypes of pericytes—'M' pericytes, characterized by the expression of extracellular matrix-maintenance genes, and 'T' pericytes, characterized by the expression of solute transporter genes—and suggested a differential association of pericyte subtypes with Alzheimer's disease.[12]

Previous studies have also linked CSVD with sleep disruption. In a post-mortem study of community-dwelling older adults, a greater burden of arteriolosclerosis, a key form of CSVD, at death was associated with greater sleep disruption.[13] Moreover, in rodent models, sleep restriction has been shown to impair pericyte structure and function.[14,15] In the rat brain, chronic sleep restriction has been shown to decrease expression of tight junction proteins and PDGFRβ and to show pericyte detachment from vessel walls.[15] Based on these observations, we hypothesized that alterations in pericyte function or subtype proportion may link sleep fragmentation to cognitive impairment in humans.

To address this question, we leveraged clinical and post-mortem data from 1270 older adult participants in two longitudinal cohort studies of ageing—the Religious Orders Study (ROS) and the Rush Memory and Aging Project (MAP). We related ante-mortem measurements of sleep fragmentation and cognitive function in the decade preceding death to post-mortem bulk tissue RNAseq. We specifically assessed the expression of marker genes for M- and T-type pericytes in the dorsolateral prefrontal cortex (DLPFC), a region associated with several cognitive abilities. To examine the extent to which region-specific effects drive these results, we also assessed pericyte subtype marker gene expression in the lateral orbitofrontal cortex (LOFC), a region associated with decision making and sleep fragmentation.[16] We tested the hypotheses that (i) sleep fragmentation is associated with the expression of pericyte subtype marker genes in the DLPFC and LOFC; and (ii) that expression of pericyte subtype marker genes is associated with cognitive trajectory in the decade before death.

Materials and methods

The methods are summarized here, and a full description can be found in the Supplementary material, 'Methods' section.

Ethics approval

The ROS and MAP studies were approved by the Institutional Review Board of Rush University Medical Center and conducted in accordance with the Declaration of Helsinki. All participants provided written informed consent and signed an anatomic gift act for brain donation and a repository consent for data sharing.

Study participants

We analysed data from 1270 older community-dwelling adults with neocortical bulk-tissue RNAseq data and cognitive assessment (1092 with RNAseq data from the DLPFC, 495 with data from the LOFC and 299 with both) participating in two longitudinal cohort studies of ageing, the MAP and the ROS.[17] Among the participants, 572 also had ante-mortem assessment of sleep fragmentation by actigraphy, and 424 had snRNAseq data from the DLPFC. Beginning in the mid-1990s, ROS recruited non-demented community-dwelling nuns, brothers and priests from across the

Table 1 Characteristics of the study population

Characteristic	Participants with DLPFC bulk RNA sequencing N = 1092	Participants with LOFC bulk RNA sequencing N = 495
Demographics		
Age at death, years	90.01 [67.37,108.28]	92.18 [70.64,108.26]
Female sex, *n* (%)	732 (67%)	360 (73%)
Years of education	16.00 [3.00,30.00]	15.00 [5.00,29.00]
Caucasian descent, *n* (%)	1076 (99%)	476 (96%)
Post-mortem interval, h	6.54 [0.87,85.08]	7.27 [3.45,40.80]
Cognition		
Mini-Mental State Examination score	25.00 [0.00,30.00]	25.00 [0.00,30.00]
Time from last cognitive assessment to death, years	0.64 [0.01,8.50]	0.66 [0.01,7.66]
Sleep		
Mean sleep fragmentation, kRA	0.03 [0.02,0.08]	0.03 [0.02,0.08]
Number of actigraphy recordings	3.00 [1.00,11.00]	4.00 [1.00,13.00]
Time from last actigraphy recording to death, years	1.74 [0.05,12.89]	2.03 [0.05,13.66]
Clinical		
Diagnosis of dementia (AD or other cause), *n* (%)	170 (41%)	195 (41%)
NIA-Reagan diagnosis of AD, *n* (%)	272 (66%)	309 (65%)
Amyloid-β coverage, % area of cortex	1.98 [0.00,4.79]	2.00 [0.00,4.79]
Neurofibrillary tangle density (per mm^2)	2.13 [0.00,8.86]	2.17 [0.00,9.01]
Presence of one or more gross chronic infarcts, *n* (%)	68/415 (16%)	83/470 (18%)
Presence of one or more chronic microinfarcts, *n* (%)	89/415 (21%)	118/470 (25%)
Moderate to severe cerebral atherosclerosis, *n* (%)	104/415 (25%)	116/473 (25%)
Mild to severe cerebral amyloid angiopathy, *n* (%)	124/414 (30%)	133/472 (28%)
Mild to severe arteriosclerosis, *n* (%)	136/413 (33%)	148/468 (32%)

Square brackets indicate [max, min]. AD = Alzheimer's disease; DLPFC = dorsolateral prefrontal cortex; LOFC = lateral orbitofrontal cortex; NIA = National Institute on Aging.

US to undergo annual clinical evaluations of myriad clinical factors, including cognitive assessments, neurological evaluations and brain donation upon death. The MAP cohort started in 1997 and recruited individuals with a wider range of life experiences and socioeconomic characteristics in the greater Chicago area to undergo the same clinical and pathological evaluations. Participant characteristics are described in Table 1, and the overlap of participants in each dataset is shown in Supplementary Fig. 1.

Identification of human pericyte subtype marker genes

As described more fully in the Supplementary material, 'Methods' section, to identify marker genes characteristic of human brain pericyte subtypes, we reanalysed published snRNAseq data from two sources.

The first source of snRNAseq data was a study by Yang *et al.*[12] of 143 793 individual nuclei from the hippocampi and frontal cortices of 17 older adults with and without Alzheimer's disease. Notably, the data were enriched for vessel-associated cell types via preprocessing with centrifugation, filtration, washing and flow cytometry, resulting in a large number of nuclei from pericytes and other vessel-associated cell types, but a paucity of non-vessel-associated cells, including neurons, astrocytes and microglia. This study identified two distinct pericyte clusters: M-type and T-type. The M-type pericyte cluster was characterized by expression of extracellular matrix-maintenance genes, including those encoding collagen and laminin proteins (Cluster 9: 5486 nuclei), while the T-type pericyte cluster was characterized by the expression of solute transporter genes (Cluster 1: 21 710 nuclei). We will refer to this study as the 'Yang' dataset.

To complement this, we additionally examined snRNAseq data from a second, complementary dataset not enriched for vessel-associated cells. This second source was a study by Green *et al.*[18] of 1 511 615 individual nuclei from the dorsolateral prefrontal cortices of 424 older adults in the ROS and MAP cohorts, 421 of which also had bulk RNA-seq data from the DLPFC. This dataset provided an opportunity to examine the extent to which genes differentiating pericytes from other vessel-associated cell types, as identified in the Yang study, also differentiate pericytes from non-vessel cell types. Clusters corresponding to pericytes were identified based on a weighted ElasticNet regularized logistic regression classifier. Two clusters of pericytes were identified and labelled 'Peri.1' (847 nuclei) and 'Peri.2' (2013 nuclei). We will refer to this study as the 'Green' dataset.

First, we confirmed the correspondence of the pericyte clusters in the Yang dataset with those in the Green dataset—M-pericytes (Cluster 9) with Peri.1 and T-pericytes (Cluster 1) with Peri.2 respectively—by examining the expression of M-pericyte (*COL4A1-4*, *ADAMTS1*, *LAMA4*) and T-pericyte (*SLC1A3*, *SLC12A7*, *SLC6A1* and *SLC20A2*) marker genes across empirically derived pericyte clusters in both snRNAseq datasets (Supplementary Fig. 2).

Next, as described in more detail in the Supplementary material, 'Methods' section, in each snRNA seq dataset, we identified candidate M-pericyte marker genes by comparing gene expression in nuclei labelled M-pericytes to all other cell type nuclei in a differential expression analysis, selecting genes that were expressed in at least 10% of nuclei and meeting an adjusted *P*-value threshold of 0.05 (Wilcoxon rank sum test). We repeated this comparison with cells labelled T-pericytes. To consider the broadest possible set of potential marker genes, we then took the union of M-pericyte marker genes identified from the Yang and Green datasets, respectively, to create a combined M-pericyte marker gene set and did the same for T-pericytes. Next, to ensure applicability to bulk RNAseq data, we excluded genes not expressed at detectable levels in our DLPFC bulk RNAseq data.

Pericytes are relatively rare in unenriched cortical tissue. Therefore, even if a pericyte marker gene is expressed at low levels in a non-pericyte cell type, expression by that cell type may nevertheless dominate bulk expression of the gene if the non-pericyte cell type is particularly abundant relative to the rarer pericytes. To guard against this, in the Green dataset, we determined the average expression for each marker gene in each major cell type (excitatory neurons, inhibitory neurons, astrocytes, oligodendroglia, microglia, macrophages, endothelial cells, smooth muscle cells) and weighted this by the relative abundance of that cell type to arrive at the weighted cell-specific expression. We included only those marker genes for which weighted pericyte-specific expression was greater than weighted expression in each of the other major cell types, so that overall bulk expression would be dominated by pericyte expression of these genes.

Next, we further filtered T- and M-pericyte marker genes based on our expectation that expression of a cell-type specific marker gene in a bulk expression sample should correlate with the relative abundance or proportion of that cell type in the sample. In other words, higher expression of a cell-type specific marker gene should correspond with a greater proportion of the cell-type in that sample relative to other samples. Therefore, we leveraged the 421 samples from the Green dataset that also had bulk RNAseq data and used beta-regression to confirm that bulk expression of each marker correlated with the proportion of nuclei of that cell type, derived from snRNAseq. We excluded candidate marker genes that were not significantly positively associated with cell type proportion at $P < 0.05$. We did this for both M-type and T-type pericytes (Supplementary Table 1).

Having identified a set of marker genes for M- and T-type pericytes, we computed a composite measure of their expression in each of the nuclei in the Green dataset. First, we centred and scaled the expression of each gene, considering all nuclei and computed the mean normalized expression of all M-pericyte marker genes in each nucleus. For each major cell type, we then computed the mean composite M-pericyte marker gene expression across all nuclei of that type. We then did the same for T-pericyte marker genes.

Next, for the 421 samples from the Green dataset that also had bulk RNAseq data, we computed a composite measure of M-pericyte marker genes in each sample using the bulk data by centring and scaling the expression of each gene considering all samples and computed the mean normalized expression of M-pericyte marker genes in each sample. We then used beta regression to relate this to the proportion of M-pericyte nuclei in each sample. We did the same for T-pericyte marker genes.

Assessment of sleep fragmentation

Sleep fragmentation was assessed biennially in the MAP cohort starting in 2005, using the metric kRA, derived from up to 10 days of continuous wrist activity monitoring. The kRA metric has previously been shown to correlate well with in-laboratory polysomnographic measures of sleep fragmentation.[19,20] kRA was developed to evaluate the probability of transition from a state of rest to a state of activity per 15-s period, after a long period of rest (~ ≥5 min). A higher kRA represents a greater degree of sleep fragmentation or interruption of sleep by arousals. Unlike other measures of sleep fragmentation, such as sleep efficiency and wake time after sleep onset, the kRA metric considers the dynamics of sleep-wake transitions and distinguishes sleep frequently interrupted by many brief arousals from sleep interrupted by one long period of wakefulness.[20] The kRA metric has previously been shown to predict incident Alzheimer's disease and cognitive decline[19] and to modify the risk of Alzheimer's disease associated with the APOE ϵ4 allele.[21] This is concordant with other studies suggesting that sleep fragmentation may be more strongly associated with cognitive risk than sleep duration.[22] Moreover, ante-mortem kRA has been associated with a number of dementia-related brain changes, including neurofibrillary tangle pathology,[21] Lewy body pathology,[23] arteriolosclerosis,[13] and microglial[24] and astrocyte activation.[25] Participants had a mean of 3.0 actigraphy recordings prior to death. Where a person had more than one measurement of sleep fragmentation prior to death, we took the average of all available measurements of sleep fragmentation, as this most accurately reflects the cumulative exposure to sleep fragmentation over the course of the study. To account for skewness in the average kRA measurements, we log-transformed the kRA data. The log-transformed kRA data were used in all downstream analyses.

Assessment of cognitive function

As described more fully in the Supplementary material, 'Methods' section, all ROS and MAP participants underwent structured annual cognitive evaluations with a battery of 19 cognitive tests assessing episodic memory, semantic memory, visuospatial ability, perceptual speed and working memory.[26] The raw scores of the cognitive tests were converted into z-scores from which an average composite z-score was obtained. Z-scores were centred at 0 (baseline performance), and negative scores indicated a decline in composite cognitive performance, while positive scores indicated an improvement. We used linear mixed-effect models to compute individual-specific rates of cognitive decline in the decade preceding death and adjusted the models for age, sex, education and post-mortem interval.

Assessment of other clinical, lifestyle, and pathologic variables

Participants' age at each annual evaluation was computed from the self-reported date of birth and the date of assessment. Age at death was computed by determining the difference in days between the self-reported date of birth and the date of death and dividing by 365.25. Years of education and sex were recorded at the time of baseline cognitive testing. The hours between the reported time of death and the time of autopsy were recorded as the post-mortem interval.

Assessments of the percentage of amyloid beta coverage in the cortex, neurofibrillary tangle pathology, diagnosis of Alzheimer's disease, presence of Lewy bodies and cerebrovascular pathologies, including presence of gross and microinfarcts, cerebral amyloid angiopathy (CAA), cerebral atherosclerosis or arteriolosclerosis, are described in the Supplementary material, 'Methods' section.

Assessment of dorsolateral prefrontal cortex gene expression

Bulk RNA sequencing was performed on frozen dorsolateral prefrontal cortex blocks from ROS and MAP participants as part of the parent study, and we leveraged these data for the current study. Detailed sequencing and pre-processing methods are described in the Supplementary material, 'Methods' section. From these data, we centered and scaled expression of the selected M- and T-pericyte marker genes across all samples and computed a composite z-score of expression by taking the mean of normalized expression.

Assessment of lateral orbitofrontal cortex gene expression

Frozen lateral orbitofrontal cortex tissue samples from MAP participants were manually dissected and homogenized for sequencing,

detailed methods of which are described in the Supplementary material, 'Methods' section. We preprocessed, normalized and batch corrected these gene expression count data using the same pipeline used for the DLPFC bulk RNAseq with minor variations described in the Supplementary material, 'Methods' section. We computed composite z-score of expression for M- and T-pericyte marker genes using the same methods as for DLPFC samples.

Statistical analysis

We sought to test two primary hypotheses: (i) sleep fragmentation is associated with composite expression of M- and T-pericyte marker genes; and (ii) composite expression of M- and T-pericyte marker genes is associated with the rate of change of composite global cognitive performance in the decade leading up to death. We implemented a false discovery rate (FDR) multiple testing correction for our four primary analyses: (i) sleep fragmentation associated with M-pericytes; (ii) M-pericytes associated with slope of cognition; (iii) sleep fragmentation associated with T-pericytes; and (iv) T-pericytes associated with slope of cognition. For all linear mixed effects and multiple linear regression models, residual plots were visually examined to confirm linearity, homoscedasticity, independence of errors and normality of errors.

First, in distinct linear regression models, we assessed the relationship between each of eight neuropathologies (amyloid-β, neurofibrillary tangles, Lewy bodies, macroscopic infarcts, microscopic infarcts, CAA, atherosclerosis, arteriolosclerosis) and M- or T-pericyte marker gene expression. We controlled for age, sex, education and post-mortem interval in these analyses to identify pathologies that could potentially confound downstream correlations with sleep and cognition. Having identified that the burden of amyloid-β pathology and severity of arteriolosclerosis correlated with M- and/or T-pericyte marker gene expression, we adjusted all subsequent models for the burden of amyloid-β pathology and severity of arteriolosclerosis.

To test the first hypothesis, we used multiple linear regression (implemented using the *lm* function in R version 4.1.0) to examine the association between average ante-mortem rest fragmentation (predictor) and composite expression of M-pericyte marker genes in our DLPFC RNAseq data (outcome) adjusted for age at death, sex, post-mortem interval, level of education, amyloid-β and arteriolosclerosis ($n = 415$). We then did the same for T-pericyte marker genes and replicated these analyses using RNAseq data from our LOFC samples. Then, we considered models augmented with terms for dementia-associated neuropathologies (amyloid-β, tangles, Lewy body pathology, large vessel atherosclerosis, arteriolosclerosis, CAA, microscopic cortical infarcts, macroscopic cortical infarcts) and also APOE genotype.

In secondary analyses, we leveraged the samples from the Green dataset who also had ante-mortem assessment of sleep fragmentation. Considering samples with at least one nucleus identified as an M-pericyte, we used multiple linear regression to examine the association between the proportion of M-pericyte nuclei in that sample (predictor) and average ante-mortem sleep fragmentation (outcome) adjusted for age, sex, level of education, and the proportion of T-pericyte nuclei.

To test our second hypothesis, we used multiple linear regression to examine the association between composite expression of M-pericyte marker genes in the DLPFC (predictor) and the rate of change of composite global cognitive function in the decade before death (outcome) adjusted for age at death, sex, level of education, source study (ROS versus MAP), amyloid-β and arteriolosclerosis ($n = 1071$ participants with complete data). We repeated these analyses with composite expression of T-pericyte marker genes as the predictor of interest. We then repeated these analyses using RNAseq data from our LOFC samples. Then, we considered models augmented with terms for dementia-associated neuropathologies (amyloid-β, tangles, Lewy body pathology, large vessel atherosclerosis, arteriolosclerosis, CAA, microscopic cortical infarcts, macroscopic cortical infarcts).

In secondary analyses, we leveraged the samples from the Green dataset who also had ante-mortem assessment of cognitive trajectory. Considering samples with at least one nucleus identified as an M-pericyte, we used multiple linear regression to examine the association between the proportion of M-pericyte nuclei in that sample (predictor) and rate of change of composite global cognitive function in the decade before death (outcome) adjusted for age, sex, level of education, and the proportion of T-pericyte nuclei.

Finally, we used the *Mediate* R package to test the hypothesis that M-pericyte gene expression mediated the association between sleep and cognitive outcomes.

Results

Study participants

We studied 1270 older community dwelling adults with neocortical bulk-tissue RNA-seq data and cognitive assessment (1092 with RNA-seq data from the DLPFC, 472 with data from the LOFC, among which 299 had both), 572 of whom also had assessment of sleep fragmentation by actigraphy. Moreover, 424 of the participants with DLPFC RNA-seq data also snRNA-seq data.[18] The characteristics of these participants are shown in Table 1.

Subtype-specific marker genes differentiate M-pericytes and T-pericytes

We reanalysed data from two recently published human brain snRNAseq datasets to identify marker genes characteristic of human brain pericyte subtypes. The first dataset, referred to as the 'Yang' dataset, sequenced 143 793 individual nuclei from the hippocampi and frontal cortices of 17 older adults with and without Alzheimer's disease, after enrichment for blood vessels, and identified two distinct subtypes of pericytes: M-pericytes and T-pericytes. The second dataset, referred to as the 'Green' dataset, sequenced 1 511 615 individual nuclei from the DLPFC of 424 older adults from the ROS and MAP cohorts, confirming clusters of pericytes expressing the M-pericyte and T-pericyte markers identified in the Yang dataset (Supplementary Fig. 2). Moreover, when we generated a combined dataset consisting of vascular niche nuclei from both the Yang and Green datasets, T-pericytes from Yang and Green overlapped substantially and did not overlap with M-pericytes from Yang and Green, which themselves overlapped substantially (Supplementary Fig. 3). Moreover, pericytes from both datasets were clearly distinct from other vascular cell types (Supplementary Fig. 4).

Differential expression analyses in the Yang and Green datasets identified a total of $n = 3735$ potential M-pericyte marker genes and $n = 2789$ potential T-pericyte marker genes differentially expressed relative to all other cell types. However, due to the relatively high abundance of non-pericyte cell types relative to pericytes, in unenriched tissue (Green dataset) weighted total expression by non-pericytes exceeded that by pericytes for the vast majority of these genes. After excluding genes where total abundance-weighted

non-pericyte expression was expected to exceed pericyte expression, and excluding genes whose bulk expression was not associated with the proportion of M- or T-pericyte nuclei in the $n = 421$ DLPFC samples with both snRNAseq and bulk RNAseq, data (Supplementary Table 1), four M-pericyte marker genes (*GJA4*, *GABRE*, *TBX15* and *TFPI*) and three T-pericyte marker genes (*CARMN*, *NOTCH3* and *FOXD1*) remained. Using a similar approach, we also generated a set of marker genes for pericytes in general.

We next examined expression of these genes in M- versus T-pericytes in the Green dataset. As expected, *GJA4*, *GABRE*, *TBX15* and *TFPI* were much more highly expressed by M-pericytes and *GABRE*, *TBX15* and *TFPI* by T-pericytes (Supplementary Fig. 5). When we examined composite expression of these genes across a larger number of cell types, expression was highest in pericytes, as expected, although there was some extra-pericyte expression in other lower abundance vascular (SMC) and blood (neutrophils, erythrocytes) cell types.

Next, in 421 DLPFC samples with both snRNAseq and bulk RNAseq data, we used beta regression to confirm that the bulk composite expression of M- and T-pericytes would be strongly correlated with the proportion of M- and T-pericyte nuclei, respectively. Indeed, this was the case, with composite expression of the M-pericyte marker genes *GJA4*, *GABRE*, *TBX15* and *TFPI* strongly predictive of the proportion of M-pericyte nuclei in each sample [estimate = +0.45, standard error (SE) = 0.05, $P = 1.1 \times 10^{-21}$; Fig. 1A], and composite expression of the T-pericyte marker genes *GABRE*, *TBX15*, and *TFPI* strongly predictive of the proportion of T-pericyte nuclei in each sample (estimate = +0.25, SE = 0.04, $P = 8.8 \times 10^{-9}$; Fig. 1C). To ensure the robustness of our finding, we repeated with analysis in only the subset of participants who had at least 1 M-pericyte ($n = 235$) or 1 T-pericyte ($n = 393$) corresponding to the subtype proportion. Despite the reduced sample size, our putative marker genes remain strongly predictive of M- and T-pericyte proportions (Supplementary Fig. 7).

When we extended this to other cell types, we found that composite expression of M- and T-pericyte gene sets much more strongly predicted the respective proportion of M- and T-pericytes than any other cell type (Supplementary Fig. 8). Notably, composite expression of the M- and T- pericyte marker genes was not associated with the proportion of SMC nuclei, which was the non-pericyte cell type that had the highest expression of these genes.

Composite expression of pericyte subtype marker genes is selectively associated with ADRD neuropathologies

We assessed the correlation between various dementia-associated neuropathologies and M-pericyte, T-pericyte, or general pericyte gene expression in $n = 1088$ participants with bulk DLPFC RNAseq data and histopathological assessment of neuropathologies. We assessed amyloid-β load (% of cortex covered), neurofibrillary tangles (cortical area mm^2), presence (versus absence) of Lewy body pathology, large vessel atherosclerosis, arteriolosclerosis, CAA, microscopic cortical infarcts, and macroscopic cortical infarcts (Table 2). Amyloid-β burden was positively associated with both M- and T-pericytes ($P < 0.05$), while arteriosclerosis was negatively associated with both pericyte subtypes ($P < 0.05$). There were no significant associations between M- or T-pericyte marker gene expression and the burden of other neuropathologies. Composite expression of marker genes for pericytes in general was lower in the presence of amyloid pathology, similar to M- and T-pericytes as noted earlier (Supplementary Table 5). Because of the potential for confounding by burden of amyloid-β or arteriolosclerosis, which in addition to being associated with pericyte marker gene expression are associated with sleep, we included both amyloid-β burden and arteriolosclerosis as covariates in downstream analyses.

We also assessed the association between APOE genotype, M- and T-pericyte expression, as well as clinical phenotypes (amyloid and tangle pathology, cognitive decline). In models adjusted for age and sex, the presence of the APOE ϵ4 allele was associated with a higher burden of amyloid and neurofibrillary tangle pathology, and with more rapid cognitive decline; However, it was not associated with the composite expression of M- and T-pericyte marker genes.

Ante-mortem sleep fragmentation associated with raised M-pericyte marker gene expression at death

We analysed data from 413 MAP participants who had measurements of both sleep fragmentation, quantified from ante-mortem actigraphy using the metric kRA, and DLPFC gene expression, quantified by bulk RNA-seq, along with documentation of post-mortem interval and dementia-associated histopathologies. In a linear regression model adjusted for age at death, sex, years of education, post-mortem interval, amyloid-β and arteriolosclerosis, greater average sleep fragmentation (log-adjusted kRA) was associated with higher composite expression of M-pericyte (estimate = +0.37, SE = 0.16, $P = 0.024$, FDR q = 0.048; Fig. 2A and Supplementary Table 2) but not T-pericyte marker genes (estimate = +0.12, SE = 0.16, $P = 0.47$, FDR q = 0.63; Fig. 2B and Supplementary Table 2). These associations remained significant in models controlling for APOE genotype. 1 standard deviation (SD) greater sleep fragmentation had a similar effect on DLPFC M-pericyte gene expression roughly equivalent to 1.7 SD greater amyloid burden.

We observed a similar result in samples from the LOFC, in which log-adjusted average kRA was positively associated with greater M-pericyte expression (estimate = +0.4, SE = 0.19, $P = 0.02$; Fig. 2C).

Pericytes accounted for <0.5% of all nuclei in the Green dataset and with ~3000–4000 nuclei per sample, many samples had only 0–5 pericyte nuclei (Supplementary Fig. 6). In secondary analyses of the small number of participants with snRNAseq data, at least one pericyte nucleus, and measurement of ante-mortem sleep fragmentation ($n = 56$), there was a positive trend between sleep fragmentation and the proportion of M-pericyte nuclei that was nevertheless concordant in direction with the results seen in our bulk RNAseq data (estimate = $+5.32 \times 10^{-1}$, SE=$+4.12 \times 10^{-1}$, $P = 0.2$; Supplementary Fig. 9A). While supportive with the bulk data, given the small number of nuclei involved, these analyses should be considered exploratory.

Multiple neurodegenerative and vascular pathologies are associated with sleep fragmentation and plausibly associated with pericyte biology. However, the association between sleep fragmentation and the composite expression of M-pericyte marker genes remained significant in both the DLPFC and LOFC in models controlling for amyloid-β burden (% of cortex covered), neurofibrillary tangles (cortical area mm^2), Lewy body pathology, large vessel atherosclerosis, arteriolosclerosis, CAA, microscopic cortical infarcts and macroscopic cortical infarcts (Supplementary Table 3).

Higher M-pericyte marker gene expression at death is related to faster ante-mortem cognitive decline

We then examined the extent to which composite expression of M- and T-pericyte marker genes in the DLPFC was associated with the rate of cognitive decline in the decade prior to death, after

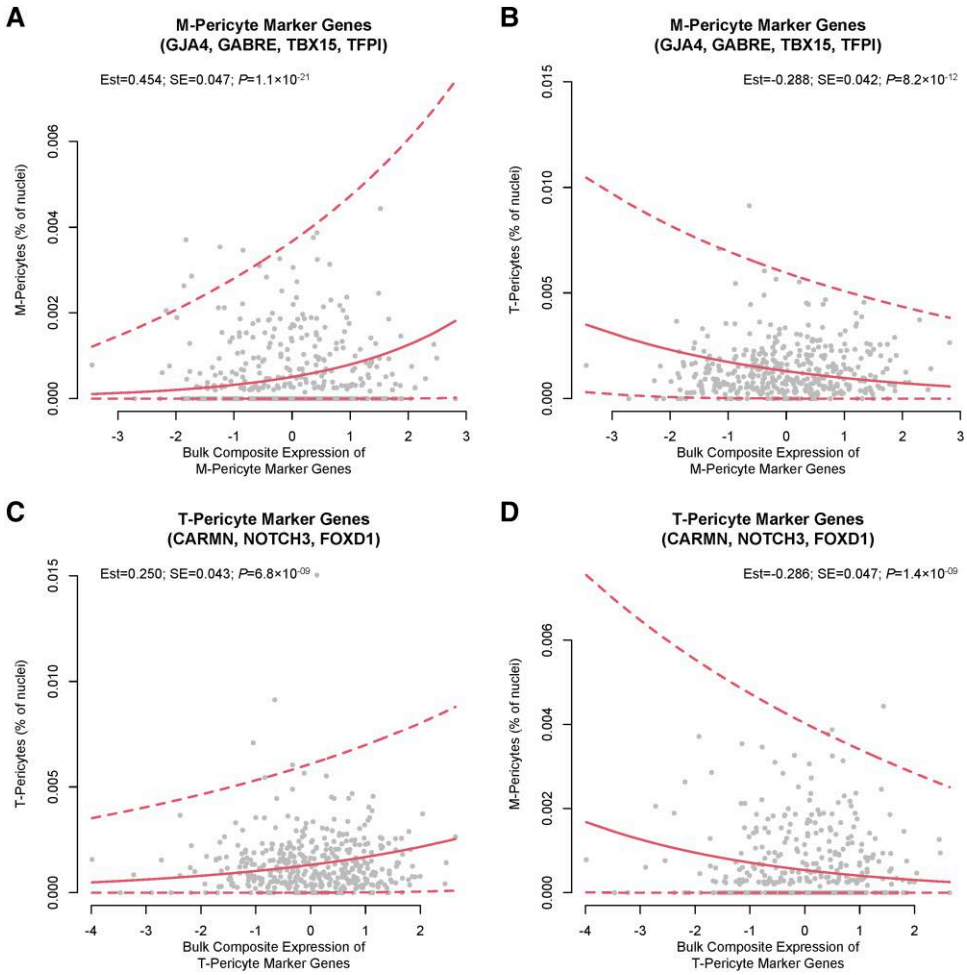

Figure 1 Bulk RNA sequencing expression of pericyte subtypes is positively correlated with same-subtype proportion and negatively correlated with contrary-subtype proportion in DLPFC data (within-subject correlations). Among the participants who were included in the DLPFC bulk RNA sequencing (RNA-seq) and sequenced in the DLPFC single-nucleus (sn)RNA-seq dataset ($n = 421$), composite expression of (**A** and **B**) M-pericyte marker genes was positively associated with the proportion of M-pericyte nuclei and negatively associated with the proportion of T-pericyte nuclei. (**C** and **D**) T-pericyte marker gene expression in bulk RNAseq was positively correlated with the proportion of T-pericyte nuclei in snRNAseq and negatively correlated with the proportion of M-pericyte nuclei. Solid line indicates best fit beta regression (with logit link), and dotted lines indicate 95% confidence intervals of the model prediction. DLPFC = dorsolateral prefrontal cortex; Est = estimate; LOFC = lateral orbitofrontal cortex; SE = standard error.

accounting for age, sex, education, post-mortem interval, study cohort, amyloid-β burden and arteriolosclerosis, in $n = 1086$ people who had complete data (including both ROS and MAP). We observed that greater expression of M-pericyte genes was associated with more rapid decline (estimate $= -8.3 \times 10^{-3}$, SE $= 3.4 \times 10^{-3}$, $P = 0.014$, FDR q = 0.048; Fig. 3A and Supplementary Table 2). In contrast, expression of T-pericyte marker genes was not associated with cognitive outcomes (estimate $= +6.5 \times 10^{-5}$, SE $= 3.5 \times 10^{-3}$, $P = 0.99$, FDR q = 0.94; Fig. 3B and Supplementary Table 2). One standard deviation greater M-pericyte gene expression was roughly equivalent to 0.35 SD greater amyloid burden in its effect on the rate of cognitive decline. This finding is replicated in the LOFC samples, in which M-pericyte marker gene expression was significantly associated with a steeper slope of change in cognition (estimate $= -1.3 \times 10^{-2}$, SE $= 4.6 \times 10^{-3}$, $P = 0.0044$; Fig. 3C). These associations remained significant in models controlling for APOE genotype.

We next sought to replicate this association using the small number of participants who had both snRNAseq data with at least one M-type and one T-type pericyte nucleus and a measurement of ante-mortem cognitive decline ($n = 200$). In this subset of participants, there was a trend towards decreased proportions of M-pericyte nuclei in the DLPFC and more rapid cognitive decline that was concordant in direction with the results seen in our bulk RNAseq data (estimate $= -1.15 \times 10^{-1}$, SE $= +7.48 \times 10^{-2}$, $P = 0.12$; Supplementary Fig. 9B). However, as with the analyses of those with sleep measurement and snRNAseq data, these analyses must be considered provisional at best.

Using the *Mediate* R package, we examined whether M-pericyte gene expression mediated the association between sleep and cognitive outcomes. These models did not provide strong statistical evidence for mediation ($P = 0.35$ for M-pericyte gene expression → sleep fragmentation → cognitive decline and $P = 0.43$ for sleep fragmentation → M-pericyte gene expression → cognitive decline), suggesting that M-pericyte gene expression and sleep fragmentation, while related, may also have independent pathways linking them to cognitive decline.

Discussion

In this study of 1270 community-dwelling older adults, higher ante-mortem sleep fragmentation was associated with greater

Table 2 Dementia-related neuropathologies and DLPFC M- and T-pericyte marker gene expression

Models				
Outcome	**Covariates**	**Estimate**	**SE**	***P* value**
M-pericytes				
–	**Amyloid-β burden (% area covered)**	$\mathbf{6.50 \times 10^{-2}}$	$\mathbf{3.09 \times 10^{-2}}$	**0.036**
–	Neurofibrillary tangle density (mm^2)	1.51×10^{-2}	3.15×10^{-2}	0.63
–	Presence of Lewy bodies	3.99×10^{-2}	3.09×10^{-2}	0.2
–	Presence of CAA	2.56×10^{-2}	3.08×10^{-2}	0.41
–	Presence of chronic microinfarcts	-7.63×10^{-3}	3.06×10^{-2}	0.8
–	Presence of gross chronic infarcts	5.71×10^{-3}	3.09×10^{-2}	0.85
–	Presence of atherosclerosis	-3.26×10^{-2}	3.07×10^{2}	0.29
–	**Presence of arteriolosclerosis**	$\mathbf{-8.03 \times 10^{-2}}$	$\mathbf{3.05 \times 10^{-2}}$	**0.0086**
T-pericytes				
–	**Amyloid-β burden (% area covered)**	$\mathbf{6.21 \times 10^{-2}}$	$\mathbf{3.09 \times 10^{-2}}$	**0.045**
–	Neurofibrillary tangle density (mm^2)	4.51×10^{-3}	3.15×10^{-2}	0.89
–	Presence of Lewy bodies	-5.79×10^{-2}	3.10×10^{-2}	0.062
–	Presence of CAA	3.25×10^{-2}	3.09×10^{-2}	0.29
–	Presence of chronic microinfarcts	1.82×10^{-2}	3.06×10^{-2}	0.55
–	Presence of gross chronic infarcts	-8.54×10^{-4}	3.09×10^{-2}	0.98
–	Presence of atherosclerosis	-1.78×10^{-2}	3.07×10^{-2}	0.56
–	**Presence of arteriolosclerosis**	$\mathbf{-6.24 \times 10^{-2}}$	$\mathbf{3.06 \times 10^{-2}}$	**0.042**

Results are linear regression models adjusted for age at death, sex, education and post-mortem interval. Covariates in bold indicate significant associations. CAA = cerebral amyloid angiopathy; SE = standard error.

expression of marker genes for M-type but not T-type pericytes in both DLPFC and LOFC. Moreover, greater expression of marker genes for M-pericytes in the DLPFC and LOFC was associated with faster residual cognitive decline over a period of 10 years prior to death, independent of age, sex, education and ADRD neuropathologies.

Identification of pericyte subtype marker genes

Leveraging two independent published human brain snRNAseq datasets, we confirmed the consistency of the division of pericytes into M- and T-type pericytes, as initially proposed by Yang and colleagues.[12] We identified *GJA4*, *GABRE*, *TFPI* and *TBX15* as putative markers of M-pericytes and *CARMN*, *FOXD1* and *NOTCH3* as putative markers of T-pericytes. While our individual genes sometimes showed expression in both M- and T-type pericytes, in the subset of samples with both snRNA-seq and bulk RNA-seq data, the bulk composite expression of these genes robustly predicted the proportion of M- and T-pericyte nuclei, respectively. Moreover, leveraging the availability of bulk and snRNAseq in a subset of samples from the Green dataset, we confirmed that composite bulk expression of these genes was associated with the abundance of M- and T-pericyte nuclei, respectively.

We note that not all recent snRNA-seq studies have found discrete clusters of transcriptionally defined M- and T-type pericytes.[27,28] This may be due to methodological differences. Winkler and colleagues[27] examined *ex vivo* tissue from individuals undergoing temporal lobectomy, who were considerably younger than the individuals in our study or in the study by Yang and colleagues.[12] Meanwhile, Garcia and colleagues[28] examined a much smaller number of samples, which may have resulted in differences in clustering pericyte subtypes. However, we note that our observations mirror the findings of a much larger snRNAseq study of ROSMAP individuals conducted subsequent to the present study, in which two distinct pericyte clusters corresponding to M- and T-pericytes were identified.[24]

Moreover, our putative M- and T-pericyte marker genes are represented in several independent snRNAseq studies of brain vascular cells. *GJA4* encodes gap junction protein a4, which forms the connexin Cx37, and its expression in pericytes is consistent with another study in mice showing high expression of GJA4 in PDGFRβ+ND2+ mural cells,[29] although in prenatal human brain tissue, *GJA4* was also found to be expressed in arterial endothelial cells.[30] The relative pericyte specificity we observed for *GJA4* in adult human brain tissue compared to antenatal brain tissue may reflect maturational changes compared to antenatal human brain. *GABRE* is the ϵ subunit of the GABA receptor. Consistent with our findings, another human brain snRNAseq study found *GABRE* to be pericyte-enriched in a subtype-specific manner.[31] Tissue factor inhibitor *TFPI* is a protease inhibitor that, outside of the brain, plays a role in regulating the blood coagulation cascade by inhibiting proteases that produce thrombin and is expressed by pericytes as well as endothelial cells.[32] *TBX15* is a transcription factor found in other studies to be expressed by human pericytes.[33,34] *CARMN* is a long non-coding RNA enriched in pericytes and smooth muscle cells enriched in one of two detected pericyte clusters in a recent snRNAseq analysis of human coronary artery.[35] Similarly, *NOTCH3* has been shown in other studies to mark human pericytes.[36]

While taken individually, some of these marker genes may be expressed by non-pericyte cell types (e.g. *NOTCH3* in pericytes and smooth muscle cells; *GABRE* in pericytes and endothelial cells). However, comparison of their composite expression across multiple cell types in the Green dataset revealed higher composite expression in pericytes than in any other cell type, including smooth muscle cells and endothelial cells. Moreover, in the samples from the Green dataset in which both bulk and snRNAseq data were available, composite expression of these marker genes was much more strongly associated with the proportion of M- and T-pericytes than with any other cell type.

One important limitation of our study is the lack of spatial information, given the important role of zonation in determining vascular cell phenotypes. For instance, pericyte morphology differs between peri-capillary pericytes and post- or pre-capillary pericytes, as does the presence or absence of smooth muscle actin.[9,37-39] However, the relationship between pericyte zonation

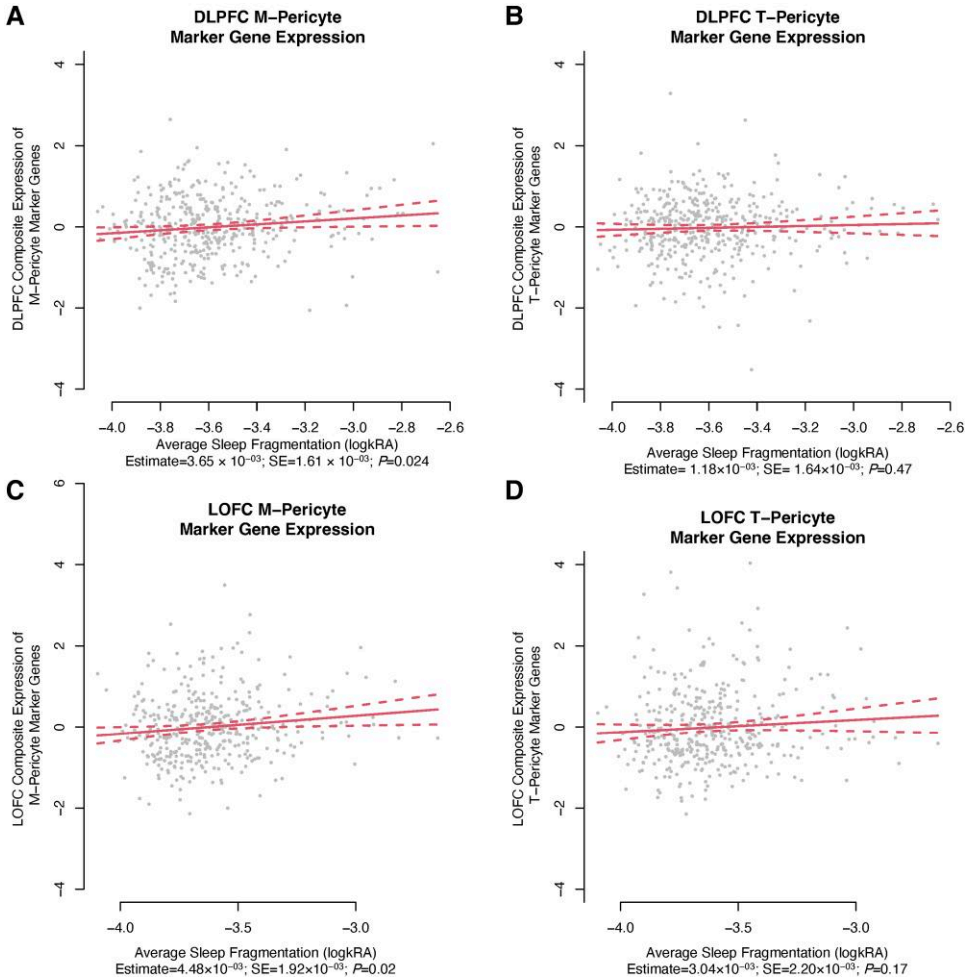

Figure 2 Ante-mortem sleep fragmentation and pericyte marker gene expression. Partial regression plots showing M-type (**A** and **C**) and T-type (**B** and **D**) pericyte marker gene expression in the DLPFC (**A** and **B**; $n = 413$) and LOFC (**C** and **D**; $n = 400$) as a function of ante-mortem sleep fragmentation (logkRA). The *y*-axis indicates composite marker gene expression, and the *x*-axis log average kRA. Each dot represents a single participant. The solid line indicates the model prediction for otherwise average participants at varying levels of sleep fragmentation, and the dotted lines indicate the 95% confidence intervals on the model prediction. All models are adjusted for age at death, sex, years of education, post-mortem interval, amyloid-β burden and presence/absence of arteriolosclerosis. DLPFC = dorsolateral prefrontal cortex; LOFC = lateral orbitofrontal cortex; SE = standard error.

and transcriptionally defined pericyte subtypes remains unclear, with some studies suggesting that the arteriovenous gradient is not a strong determinant of pericyte transcriptional phenotypes.[28] Additional studies employing spatial transcriptomic approaches are needed to better characterize the relationship between sleep, pericyte transcriptomes, zonation and cognitive decline.

Dementia-associated neuropathologies and expression of M- and T-pericyte marker genes

There is considerable evidence for a link between Alzheimer's disease pathogenesis and vascular brain pathology. Brains from patients with Alzheimer's disease show histological evidence of altered vessel structure and morphology and disruption of the basement membrane and BBB.[40,41] Deposition of amyloid-β on arterial walls, cerebral amyloid angiopathy, is also seen.[42] TgCRND8 transgenic mice show depletion of mural cells, including pericytes, covering both arterioles and venules, which is accompanied by abnormalities of functional hyperaemia, with further aberrant morphology with pharmacological depletion of pericytes.[43]

We observed that a greater severity of arteriolosclerosis was associated with lower expression of both M- and T-pericyte marker genes. This is not surprising, since damage to blood vessel walls is plausibly accompanied by fewer pericytes. Meanwhile, the positive association between amyloid-β pathology and greater relative expression of M- and T-pericyte marker genes is, on the surface, somewhat surprising. This may reflect an impact of amyloid-β pathology on reducing the numbers of other types of cells, such as neurons, even more than pericytes, resulting in a relatively greater abundance of pericytes that manifests as pericyte marker genes accounting for a greater proportion of overall RNA.

Higher ante-mortem sleep fragmentation is associated with greater expression of M-pericyte marker genes

In this study, higher ante-mortem sleep fragmentation, measured by actigraphy, was associated with greater expression of M-pericyte marker genes in both DLPFC and LOFC. This relationship remained significant after controlling for factors such as age, sex and education, as well as a host of dementia-associated neuropathologies. Moreover, a similar association was not seen with T-pericyte marker genes, indicating a degree of subtype specificity.

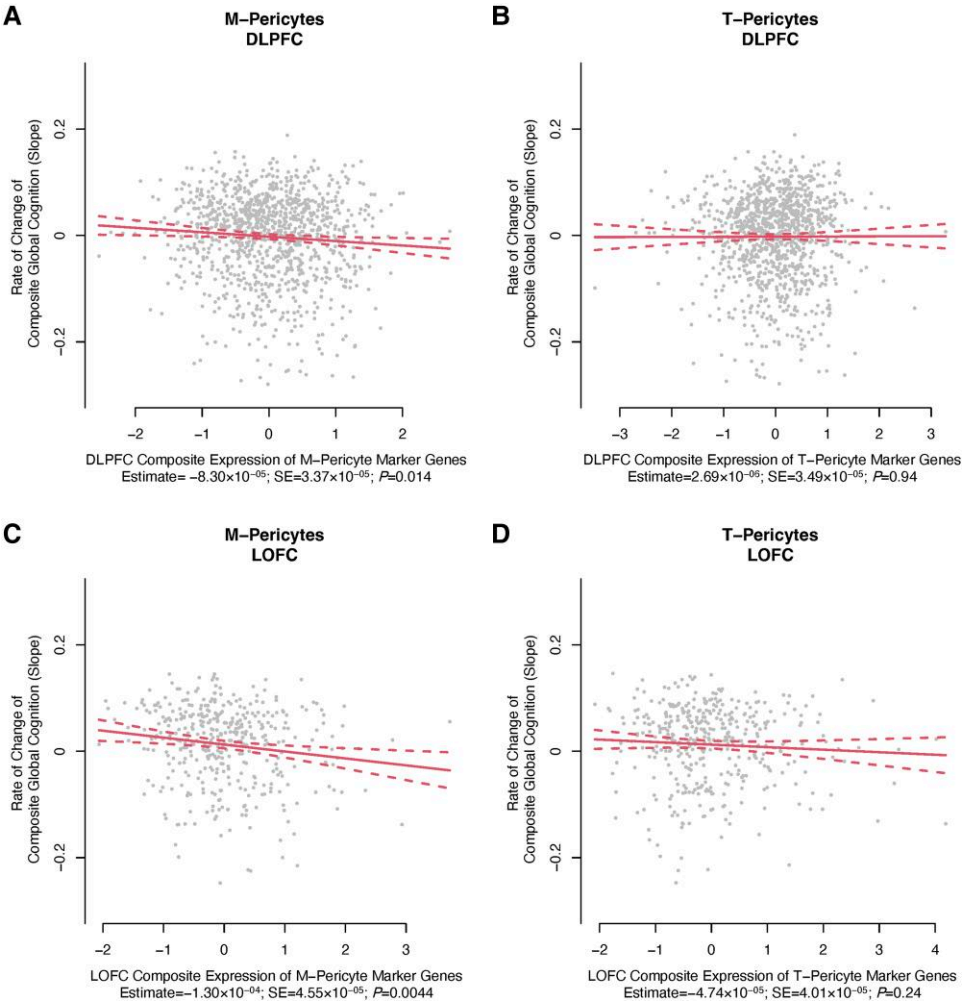

Figure 3 Pericyte marker gene expression and rate of cognitive decline in the decade before death. Partial regression plots showing individual-specific rate of cognitive decline as a function of M-type (**A** and **C**) and T-type (**B** and **D**) pericyte marker gene expression in the DLPFC (**A** and **B**; $n = 1071$) and LOFC (**C** and **D**; $n = 403$). The *y*-axis indicates the rate of cognitive decline, and the *x*-axis the composite expression of M- or T-pericyte marker genes. Each dot represents a single participant. The solid line indicates the model prediction for otherwise average participants at varying levels of composite gene expression, and the dotted lines indicate the 95% confidence intervals on the model prediction. All models are adjusted for age at death, sex, years of education, post-mortem interval, amyloid-β burden and presence/absence of arteriolosclerosis. DLPFC = dorsolateral prefrontal cortex; LOFC = lateral orbitofrontal cortex; SE = standard error.

As our study was ultimately cross-sectional in nature, we cannot conclude whether sleep fragmentation is a contributor to, or result of, a greater proportion of M-pericytes. However, in the rat brain, chronic sleep restriction has been shown to decrease the expression of tight junction proteins and PDGFR-β and pericyte detachment from vessel walls,[15] supporting a possible effect of sleep disruption on pericyte biology. On the other hand, pericytes play an important role in BBB function. In humans, other causes of differences in BBB function (e.g. polymorphisms in aquaporin 4) are associated with differences in sleep depth measured by EEG,[44] suggesting that alterations in pericyte biology may also affect sleep architecture.

Higher M-pericyte marker gene expression correlates with worse cognitive function and faster decline

Greater expression of M-pericyte marker genes in both the DLPFC and the LOFC was associated with a steeper rate of cognitive decline in the decade leading to death in community-dwelling older adults. This was independent of age, sex, education and dementia-associated neuropathologies. T-pericyte marker gene expression was not similarly associated with ante-mortem cognitive function, suggesting subtype specificity. As with our findings with sleep, we observed a concordant, but non-significant, association between greater ante-mortem sleep fragmentation and the proportion of M-pericyte nuclei in a subset of samples with both ante-mortem cognitive data and snRNAseq. Other studies have noted associations between pericyte subtype proportions and Alzheimer's disease, which in turn is associated with cognitive impairment.[12,31] However, in one of these studies, the proportion of M-pericytes was lower, rather than higher, in patients with Alzheimer's disease compared to cognitively normal adults. While, on the surface, these results may appear discrepant with our finding that higher expression of M-pericyte marker genes is associated with faster cognitive decline, we think there are several ways to reconcile these results. First, we controlled for the burden of amyloid-β pathology in our analyses such that for a given burden of amyloid-β pathology, higher expression of M-pericyte marker genes was associated with more rapid decline. Second, rather than

selecting specifically for cognitive impairment due to Alzheimer's disease pathology, we included a broad spectrum of causes of cognitive impairment. It is possible that higher expression of M-pericytes is associated with non-Alzheimer's disease-related pathways towards cognitive impairment, such as the 'alternative brain ageing' pathway proposed by Green *et al.*,[18] which is characterized by reactive microglia and astrocytes, among other cellular changes. Third, whereas the study by Yang and colleagues[12] enriched for vessel-associated cells, we studied bulk tissue RNA-seq, which may represent different tissue compartments—it is possible that M-pericytes may increase in one compartment even while decreasing in another.

Whether the relatively greater expression of M- versus T-pericyte marker gene expression in those with faster cognitive decline reflects more M-type or fewer T-type pericytes is impossible to conclude from our bulk RNA-seq data. To account for between-sample differences in RNA concentration, bulk RNA data were normalized to the transcriptome as a whole. Therefore, a relative increase in M-pericytes and a relative decrease in T-pericytes may look the same after normalization. Thus, preferential loss of T-type pericytes, for instance, due to preferential damage to vessels ensheathed by them, could potentially account for the apparent enrichment for M-type pericytes in those with the fastest cognitive impairment. Additional histological or spatial transcriptomic studies assessing the density per unit area of specific pericyte subtypes will help determine whether differential damage to spatially defined vessel subgroups drives the apparent differential relationship between M- and T-type pericytes and cognitive decline.

It is also impossible to conclude whether the shift in pericyte subtypes in those with the fastest cognitive decline plays a causal role in that decline or is simply a consequence of an underlying causally important mechanism. If this shift is indeed causal, then altered BBB function may be a potential mediating mechanism. Pericyte-deficient mice have aberrant BBB function,[45] and in humans, CSF levels of the pericyte marker PDGFRβ coincide with increased BBB permeability in the hippocampus as measured by dynamic contrast-enhanced MRI.[10] Moreover, increased BBB permeability may be present even in the earliest stages of Alzheimer's disease pathogenesis.[46]

Methodological considerations

Despite the statistically robust findings present here, several limitations merit discussion. First, owing to the relatively small number of samples with both snRNAseq data and our phenotypes of interest, our primary analyses were carried out using bulk RNAseq data. Accordingly, it is impossible to exclude the possibility that the observed results may have been partly driven by non-pericyte expression of these marker genes, particularly by endothelial cells, smooth muscle cells and fibroblasts, given the non-zero expression we observed in these cell types. Mitigating against this, in our direct comparisons of bulk expression of these marker genes with the proportion of nuclei in samples with both snRNAseq and bulk RNAseq, pericyte marker gene expression was much more strongly associated with the proportion of M- and T-type pericytes than with other cell types. Moreover, when we directly examined associations with sleep and cognition in the subset of samples with snRNAseq data, we saw relationships concordant with our analyses of the bulk RNAseq data, although these were statistically non-significant. Replication of our results in larger snRNAseq datasets with sleep measurement is needed. Second, our cross-sectional design precludes causal inference. Longitudinal studies or controlled experiments relating change in sleep fragmentation to change in biomarkers of pericyte biology (e.g. CSF PDGFRβ) may be helpful. Third, we acknowledge that kRA measured by actigraphy is only a proxy for sleep fragmentation measured by cumbersome methods like polysomnography and cannot distinguish causes of sleep fragmentation (such as sleep apnoea, environmental disturbances such as noise or sleep disorders). Studies using more physiologically detailed methods of sleep phenotyping would be helpful. Fourth, we studied predominantly older women of European ancestry. Additional studies in other populations are needed to confirm generalizability.

There are also several strengths to our approach in this study. First, we derived our marker gene sets from two independent published human snRNAseq datasets, which were largely concordant in identifying the transcriptional phenotypes of M- and T-type pericytes. Second, we were able to leverage a subset of samples with both snRNAseq and bulk RNAseq data to confirm the strong selective association between bulk expression of our M- and T-pericyte marker genes and the proportion of M- and T-pericyte nuclei. Third, we used actigraphy as an objective measure of sleep fragmentation, avoiding issues raised by self-report measures, including poor recall and poor correlation with polysomnography. Fourth, we accounted for a wide range of dementia-associated neuropathologies directly quantified by histopathology.

Future directions and clinical implications

Our study raises the possibility that changes in pericyte subpopulations, specifically a shift towards M-pericytes, may be a mechanism linking sleep fragmentation with small vessel disease and cognitive decline. If confirmed in model organisms and clinical trials of sleep interventions with pericyte biomarker outcomes (e.g. CSF PDGFRβ), it would highlight that sleep interventions may be an effective means to alter human small vessel biology and cognitive decline. It also raises the possibility that aggressive treatment of other risk factors for cerebral small vessel disease may help prevent the deleterious impact of sleep fragmentation on small vessel biology.

Data availability

The snRNAseq dataset published by Yang *et al.*[12] is deposited in the NCBI Gene Expression Omnibus under accession code GSE163577 and available to download from https://cells–test.gi.ucsc.edu/?ds=brain. The snRNAseq dataset from Green *et al.*[18] was provided courtesy of the deJager lab at Columbia University. The dataset is available upon reasonable request on synapse.org (ID: syn34572333). DLPFC bulk RNAseq data have been deposited on synapse.org. LOFC bulk RNAseq data will be deposited on synapse.org upon publication. ROSMAP data can be requested at www.radc.rush.edu.

Acknowledgements

We thank the participants of the ROS and MAP studies for their contribution and brain donation. We also thank Dr JoAnne McLaurin and Dr Sandra Black for their insight and feedback.

Funding

This study was supported by grants from the National Institute on Aging [R01AG070436, R01AG052488, RF1AG036042, R01AG048015, U01AG061356, R01AG15819, R01AG017917, R01AG047976,

R01AG056352, R01AG024480, RF1AG070438, U01AG072572, R01AG074082, R01AG079223] The Natural Sciences and Engineering Research Council of Canada (RGPIN-2020-05834 and DGECR-2020-00048], The Robert C. Borwell Endowment Fund and the Krembil Foundation.

Competing interests

The authors report no competing interests.

Supplementary material

Supplementary material is available at *Brain* online.

References

1. WHO. Dementia. Accessed 31 March 2023. https://www.who.int/news-room/fact-sheets/detail/dementia.
2. Hauglund NL, Pavan C, Nedergaard M. Cleaning the sleeping brain—The potential restorative function of the glymphatic system. *Curr Opin Physiol*. 2020;15:1-6.
3. Wang C, Holtzman DM. Bidirectional relationship between sleep and Alzheimer's disease: Role of amyloid, tau, and other factors. *Neuropsychopharmacology*. 2019;45:104-120.
4. Zhang F, Zhong R, Li S, et al. Alteration in sleep architecture and electroencephalogram as an early sign of Alzheimer's disease preceding the disease pathology and cognitive decline. *Alzheimers Dement*. 2019;15:590-597.
5. Khosroazad S, Abedi A, Hayes MJ. Sleep signal analysis for early detection of Alzheimer's Disease and Related Dementia (ADRD). *IEEE J Biomed Health Inform*. 2023;27:2264-2275.
6. Evans LE, Taylor JL, Smith CJ, Pritchard HAT, Greenstein AS, Allan SM. Cardiovascular comorbidities, inflammation, and cerebral small vessel disease. *Cardiovasc Res*. 2021;117:2575-2588.
7. Mu R, Qin X, Guo Z, et al. Prevalence and consequences of cerebral small vessel diseases: A cross-sectional study based on community people plotted against 5-year age strata. *Neuropsychiatr Dis Treat*. 2022;18:499-512.
8. Brown LS, Foster CG, Courtney JM, King NE, Howells DW, Sutherland BA. Pericytes and neurovascular function in the healthy and diseased brain. *Front Cell Neurosci*. 2019;13:282.
9. Uemura MT, Maki T, Ihara M, Lee VMY, Trojanowski JQ. Brain microvascular pericytes in vascular cognitive impairment and dementia. *Front Aging Neurosci*. 2020;12:80.
10. Nation DA, Sweeney MD, Montagne A, et al. Blood–brain barrier breakdown is an early biomarker of human cognitive dysfunction. *Nat Med*. 2019;25:270-276.
11. Sweeney MD, Montagne A, Sagare AP, et al. Vascular dysfunction—The disregarded partner of Alzheimer's disease. *Alzheimers Dement*. 2019;15:158-167.
12. Yang AC, Vest RT, Kern F, et al. A human brain vascular atlas reveals diverse mediators of Alzheimer's risk. *Nature*. 2022;603:885-892.
13. Lim ASP, Yu L, Schneider JA, Bennett DA, Buchman AS. Sleep fragmentation, cerebral arteriolosclerosis, and brain infarct pathology in community-dwelling older people. *Stroke*. 2016;47:516.
14. Hurtado-Alvarado G, Cabañas-Morales AM, Gómez-Gónzalez B. Pericytes: Brain-immune interface modulators. *Front Integr Neurosci*. 2014;7(JAN):80.
15. Medina-Flores F, Hurtado-Alvarado G, Contis-Montes de Oca A, et al. Sleep loss disrupts pericyte-brain endothelial cell interactions impairing blood-brain barrier function. *Brain Behav Immun*. 2020;89:118-132.
16. Lim ASP, Fleischman DA, Dawe RJ, et al. Regional neocortical gray matter structure and sleep fragmentation in older adults. *Sleep*. 2016;39:227-235.
17. Bennett DA, Buchman AS, Boyle PA, Barnes LL, Wilson RS, Schneider JA. Religious orders study and rush memory and aging project. *J Alzheimers Dis*. 2018;64(Suppl 1):S161.
18. Green GS, Fujita M, Yang H-S, et al. Cellular communities reveal trajectories of brain ageing and Alzheimer's disease. *Nature*. 2024;633:634-645.
19. Lim ASP, Kowgier M, Yu L, Buchman AS, Bennett DA. Sleep fragmentation and the risk of incident Alzheimer's disease and cognitive decline in older persons. *Sleep*. 2013;36:1027.
20. Lim ASP, Yu L, Costa MD, et al. Quantification of the fragmentation of rest-activity patterns in elderly individuals using a state transition analysis. *Sleep*. 2011;34:1569-1581.
21. Lim ASP, Yu L, Kowgier M, Schneider JA, Buchman AS, Bennett DA. Modification of the relationship of the apolipoprotein E ϵ4 allele to the risk of Alzheimer disease and neurofibrillary tangle density by sleep. *JAMA Neurol*. 2013;70:1544-1551.
22. Leng Y, Knutson K, Carnethon MR, Yaffe K. Association between sleep quantity and quality in early adulthood with cognitive function in midlife. *Neurology*. 2024;102:e208056.
23. Sohail S, Yu L, Schneider JA, Bennett DA, Buchman AS, Lim ASP. Sleep fragmentation and Parkinson's disease pathology in older adults without Parkinson's disease. *Mov Disord*. 2017;32:1729-1737.
24. Kaneshwaran K, Olah M, Tasaki S, et al. Sleep fragmentation, microglial aging, and cognitive impairment in adults with and without Alzheimer's dementia. *Sci Adv*. 2019;5:eaax7331.
25. Wu R, Tripathy S, Menon V, et al. Fragmentation of rest periods, astrocyte activation, and cognitive decline in older adults with and without Alzheimer's disease. *Alzheimers Dement*. 2023;19:1888-1900.
26. Wilson RS, Boyle PA, Yu L, et al. Temporal course and pathologic basis of unawareness of memory loss in dementia. *Neurology*. 2015;85:984.
27. Winkler EA, Kim CN, Ross JM, et al. Single cell atlas of the normal and malformed human brain vasculature. *Science*. 2022;375:eabi7377.
28. Garcia FJ, Sun N, Lee H, et al. Single-cell dissection of the human brain vasculature. *Nature*. 2022;603:893-899.
29. He L, Vanlandewijck M, Raschperger E, et al. Analysis of the brain mural cell transcriptome. *Sci Rep*. 2016;6:35108.
30. Crouch EE, Bhaduri A, Andrews MG, et al. Ensembles of endothelial and mural cells promote angiogenesis in prenatal human brain. *Cell*. 2022;185:3753-3769.e18.
31. Sun N, Akay LA, Murdock MH, et al. Single-cell multi-region dissection of brain vasculature in Alzheimer's Disease. *Nat. Neurosci*. 2023;226:970-82. Erratum in: *Nat. Neurosci*. 2023;26:2251.
32. Crawley J, Lupu F, Westmuckett AD, Severs NJ, Kakkar VV, Lupu C. Expression, localization, and activity of tissue factor pathway inhibitor in normal and atherosclerotic human vessels. *Arterioscler Thromb Vasc Biol*. 2000;20:1362-1373.
33. Guijarro-Muñoz I, Compte M, Álvarez-Cienfuegos A, Álvarez-Vallina L, Sanz L. Lipopolysaccharide activates toll-like receptor 4 (TLR4)-mediated NF-κB signaling pathway and proinflammatory response in human pericytes. *J Biol Chem*. 2014;289:2457-2468.
34. da Silva Meirelles L, de Deus Wagatsuma VM, Malta TM, et al. The gene expression profile of non-cultured, highly purified human adipose tissue pericytes: Transcriptomic evidence that pericytes are stem cells in human adipose tissue. *Exp Cell Res*. 2016;349:239-254.

35. Dong K, Shen J, He X, et al. CARMN is an evolutionarily conserved smooth muscle cell-specific LncRNA that maintains contractile phenotype by binding myocardin. *Circulation*. 2021;144: 1856-1875.
36. Jäkel S, Agirre E, Mendanha Falcão A, et al. Altered human oligodendrocyte heterogeneity in multiple sclerosis. *Nature*. 2019; 566:543-547.
37. Alarcon-Martinez L, Shiga Y, Villafranca-Baughman D, et al. Pericyte dysfunction and loss of interpericyte tunneling nanotubes promote neurovascular deficits in glaucoma. *Proc Natl Acad Sci U S A*. 2022;119:e2110329119.
38. Nehls V, Drenckhahn D. Heterogeneity of microvascular pericytes for smooth muscle type alpha-actin. *J Cell Biol*. 1991;113: 147-154.
39. Alarcon-Martinez L, Yemisci M, Dalkara T. Pericyte morphology and function. *Histol Histopathol*. 2021;36:633-643.
40. Fisher RA, Miners JS, Love S. Pathological changes within the cerebral vasculature in Alzheimer's disease: New perspectives. *Brain Pathol*. 2022;32:e13061.
41. Kalaria RN, Mori H, Hedera P. Amyloid β protein and the cerebrovascular pathology in Alzheimer's disease. *Neurobiol Aging*. 1996;4:S39.
42. Attems J, Jellinger KA. The overlap between vascular disease and Alzheimer's disease-lessons from pathology. *BMC Med*. 2014;12:1-2.
43. Lai AY, Dorr A, Thomason LAM, et al. Venular degeneration leads to vascular dysfunction in a transgenic model of Alzheimer's disease. *Brain*. 2015;138:1046-1058.
44. Ulv Larsen SM, Landolt H-P, Berger W, Nedergaard M, Knudsen GM, Holst SC. Haplotype of the astrocytic water channel AQP4 is associated with slow wave energy regulation in human NREM sleep. *PLoS Biol*. 2020;18:e3000623.
45. Bell RD, Winkler EA, Sagare AP, et al. Pericytes control key neurovascular functions and neuronal phenotype in the adult brain and during brain aging. *Neuron*. 2010;68:409-427.
46. Montagne A, Nation DA, Sagare AP, et al. APOE4 leads to blood-brain barrier dysfunction predicting cognitive decline. *Nature*. 2020;581:71-76.